JGR Space Physics

RESEARCH ARTICLE
10.1029/2021JA029388

Key Points:

- The re-reconnection between two flux ropes (FRs) results in a transformation of free field lines into semi-open field lines
- The re-reconnection between a FR and cusp field lines produces more semi-open field lines, and the FR can break into two short ones
- The two re-reconnection processes favor particle/energy transport toward Earth's magnetosphere, which may affect poleward moving auroral forms (PMAFs)

Correspondence to:
S. Lu and Q. M. Lu,
lusan@ustc.edu.cn;
qmlu@ustc.edu.cn

Citation:
Guo, J., Lu, S., Lu, Q., Lin, Y., Wang, X., Huang, K., et al. (2021). Re-reconnection processes of magnetopause flux ropes: Three-dimensional global hybrid simulations. *Journal of Geophysical Research: Space Physics*, *126*, e2021JA029388. https://doi.org/10.1029/2021JA029388

Received 1 APR 2021
Accepted 25 MAY 2021

Re-Reconnection Processes of Magnetopause Flux Ropes: Three-Dimensional Global Hybrid Simulations

Jin Guo[1,2], San Lu[1,2], Quanming Lu[1,2], Yu Lin[3], Xueyi Wang[3], Kai Huang[1,2], Rongsheng Wang[1,2], and Shui Wang[1,2]

[1]CAS Key Lab of Geospace Environment, School of Earth and Space Sciences, University of Science and Technology of China, Hefei, Anhui, China, [2]CAS Center for Excellence in Comparative Planetology, Hefei, Anhui, China, [3]Physics Department, Auburn University, Auburn, AL, USA

Abstract Magnetopause flux ropes (FRs) play a crucial role in the transport of energy and plasma from the solar wind to the Earth's magnetosphere. Once formed by multiple X-line reconnection, the FRs move poleward, during which they can coalesce with each other through a re-reconnection process. The poleward moving FRs eventually coalesce into the cusp regions, through another re-reconnection process. In this paper, using three-dimensional (3-D) global hybrid simulations, we study the two re-reconnection processes of magnetopause FRs by examining the topological changes of magnetic field lines. These re-reconnection processes are essentially 3-D. Two FRs coalesce with each other and form two new FRs (instead of one new FR in the two-dimensional regime). When FRs move close to the cusp region, their field lines can reconnect with the cusp field lines so that the FRs can break into two shorter ones. The two re-reconnection processes increase the plasma energy and the magnetic flux connected to the Earth, which favors particle and energy transport toward the Earth's magnetosphere.

1. Introduction

Flux ropes (FRs) are magnetic structures composed of helical magnetic field lines, which are universal in space. The FRs act as flux transfer events (FTEs) at the Earth's magnetopause (e.g., Russell & Elphic, 1978), plasmoids in the magnetotail (Zong et al., 2004), and coronal mass ejection in the heliosphere (Ruffenach et al., 2012). Earth's magnetopause FRs play an important role in the transfer of energy and plasma from the solar wind into the magnetosphere during the southward interplanetary magnetic field (IMF). Russell and Elphic (1978) first observed the FTEs, and they believe that FTEs are elbow-shaped magnetopause flux tubes formed by magnetopause reconnection. Lee and Fu (1985) proposed that magnetopause multiple X line reconnection can form FTEs as magnetic FRs with helical internal structure. In the following decades, based on the spacecraft observations and theories, the configuration, size, evolution, and inner structure of the magnetopause FRs were studied extensively (e.g., Akhavan-Tafti et al., 2018; Chen et al., 2017; Fuselier et al., 2018; Hasegawa et al., 2010; Øieroset et al., 2016; Omidi & Sibeck, 2007; Tan et al., 2011; Wang et al., 2017; Zhong et al., 2013). These results show that the FTEs are essentially FRs with helical magnetic structure.

After being formed by the multiple X line reconnection process (considered as the primary reconnection process), the FRs can coalesce with each other through a re-reconnection process, which releases a large amount of energy (e.g., Oka et al., 2010; Pritchett, 2008; Wang, Lu, Huang, & Wang, 2016). Recently, the coalescence of FRs has been observed both at the Earth's magnetopause (Alm et al., 2018; Kacem et al., 2018; Øieroset et al., 2016; Wang et al., 2017; Zhou et al., 2017) and in Earth's magnetotail (Wang, Lu, Nakamura, et al., 2016). Two-dimensional global hybrid simulations, which assume uniformity and infinite length in the dawn-dusk direction, have shown that small magnetopause FRs can coalesce with each other near the subsolar point (Hoilijoki et al., 2017; Sibeck & Omidi, 2012). However, the magnetopause FRs are three-dimensional (3-D) in nature. Previously, Tan et al. (2011) studied the magnetopause reconnection and FRs with southward IMF, and Tan et al. (2012) studied ion cusp precipitation associated with magnetopause reconnection. Moreover, Guo et al. (2020) study the formation and global evolution of magnetopause FRs in a Magnetospheric Multiscale (MMS) event with dipole tilt.

The formation and evolution of the magnetopause FRs are controlled by the IMF clock angle. Using 3-D global hybrid simulations, Guo et al. (2021) studied the 3-D structures and evolution of FRs formed by

magnetopause reconnection with different southward IMF clock angles, and they found that whether and where FR coalescence occurs are controlled by the IMF clock angle. However, the detailed coalescence process, that is, the topological change of magnetic field lines during the re-reconnection, is still unclear.

FRs are formed at the low-latitude magnetopause with a pure southward IMF, and then they gradually move poleward toward the cusp regions at an Alfvénic speed (Guo et al., 2020; Sibeck & Omidi, 2012; Tan et al., 2011). When the FRs enter the cusp, their field lines can reconnect with the cusp magnetic field lines (i.e., tail lobe magnetic field lines) through another kind of re-reconnection (Omidi & Sibeck call it secondary reconnection), during which the plasma in the FRs can enter the ionosphere, as shown by the 2-D global hybrid simulations in Omidi and Sibeck (2007). However, the axial (west-east) length of FRs can reach more than a dozen R_E (where R_E is the Earth's radius, Guo et al., 2021). The structure and nature of the re-reconnection between FR and cusp field lines in 3-D is also unclear.

Therefore, the purpose of this study is to address the above two re-reconnection processes of the magnetopause FRs, (a) the coalescence of FRs and (b) reconnection between FRs and cusp magnetic field lines in 3-D. In this paper, we use 3-D global hybrid simulations to examine the 3-D topological change of magnetic field lines in the two re-reconnection processes. Section 2 is the description of the simulation model, Section 3 is the simulation results, and the Section 4 contains the conclusions and discussion.

2. Simulation Model

Hybrid simulations treat ions as particles and electrons as a massless, charge-neutralizing fluid. In this paper, the global hybrid simulation scheme (Lin & Wang, 2005; Swift, 1996) is used to study the re-reconnection of dayside magnetopause FRs. The geocentric solar-magnetospheric (GSM) coordinate is employed to describe the simulation results, in which the x axis points from the Earth to the Sun, the z axis points to the Earth's northern magnetic pole, and the y axis completes the right-handed system.

In the simulation, a spherical coordinate system is used. In the conventional spherical coordinate system, the polar angle θ ($0° \le \theta \le 180°$) is measured from the positive GSM z axis, and the azimuthal (longitudinal) angle φ ($0° \le \varphi \le 360°$) from the negative GSM y axis. To avoid the singular coordinate line along the polar axes, a semicone polar angle around the positive and negative polar axes is cut out from the domain, and the positive and negative polar axes are chosen along the GSM $\pm y$ axes in the calculation (Lin &Wang, 2006). While cutting a semicone polar angle around the positive and negative polar axes, the dayside cusps can be retained due to rotation of the polar axis to the y axis (Lin &Wang, 2005). However, for the presentation in the following, we use the conventional spherical coordinate system to describe the simulation domain. The bow shock, magnetosheath, and magnetosphere in the dayside region are all contained in the simulation domain.

The IMF clock angle α is defined as the angle between the GSM-z and projection of IMF in the GSM y-z plane, and the IMF is assumed to be $\mathrm{B}_0 = \left(B_{x0}, B_{y0}, B_{z0}\right) = \left(0, \sin\alpha, \cos\alpha\right) B_0$. Two cases with different initial parameters are presented in this paper. Case 1 has $\alpha = 150°$, $B_{y0} = 0.5B_0$, and $B_{z0} = -0.8660B_0$, and its simulation domain includes a geocentric distance $4\ R_E \le r \le 24\ R_E$, polar angle $0° < \theta < 180°$ and azimuth angle $20° < \varphi < 160°$; Case 2 has $\alpha = 225°$, $B_{y0} = -0.7071B_0$, and $B_{z0} = -0.7071B_0$, and its simulation domain includes a geocentric distance $4\ R_E \le r \le 27\ R_E$. For this case, the simulation domain is extended tailward by a 10° angle from the $x = 0$ plane around the y axis for both $z > 0$ and $z < 0$, and thus more cusp region can be contained. A total grid $N_r \times N_\varphi \times N_\theta = 220 \times 114 \times 130$ and $N_r \times N_\varphi \times N_\theta = 400 \times 200 \times 200$ is used in Cases 1 and 2, respectively. To produce a higher resolution near the magnetopause, nonuniform grids are used in the r direction with a smaller grid size of $\Delta r \approx 0.03\ R_E$ limited to $8\ R_E \le r \le 10\ R_E$ and $8\ R_E \le r \le 14\ R_E$ in Cases 1 and 2, respectively. The Earth is located at the origin, $r = 0$. Outflow boundary conditions are utilized at the tailward boundary at $x = 0$, and solar wind inflow boundary conditions are applied for the outer boundary at $r = 24\,R_E$ and $27\,R_E$ in Cases 1 and 2, respectively. The inner boundary at $r = 4\,R_E$ in Cases 1 and 2, is perfectly conducting. The ions are fully kinetic particles in our hybrid simulation model, but the ions in the inner magnetosphere ($r < 7\,R_E$) are treated as a cold fluid. Initially, the Earth's dipole magnetic field is limited to $r \le 10\ R_E$, and it interacts with the uniform solar wind placed in $r > 10\ R_E$. The time step is $\Delta t = 0.05\Omega_{i0}^{-1}$.

A small current-dependent collision frequency ($\upsilon = 0.02\Omega_i J \,/\, J_0$) is used to simulate the anomalous resistivity (e.g., Lin et al., 2014) and trigger magnetic reconnection at the magnetopause, where J is the current density, Ω_i is the local ion gyro-frequency and $J_0 = B_0 \,/\, \mu_0 d_{i0}$ The anomalous resistivity is usually attributed to particle kinetic effects, especially that of the electrons, such as electron nongyrotropy (e.g., Kuznetsova et al., 1998) and/or turbulent wave-particle interaction (e.g., Che et al., 2011). The ion and electron plasma beta in the solar wind is $\beta_i = \beta_e = 0.5$, and the Alfvén Mach number M_A is 5. The ion number density in the solar wind is set to be $N_0 = 11000\ R_E^{-3}$ ($N_0 = 10000\ R_E^{-3}$ in Case 2). After the simulations begin, the solar wind plasma will flow into the simulation domain along the -x direction with an isotropic drifting-Maxwellian distribution.

In our simulations, the magnetic field and ion number density are normalized by the IMF magnitude B_0 and the solar wind density N_0, respectively; The flow velocity is normalized by the solar wind Alfvén speed $V_{A0} = B_0 \,/\, \sqrt{\mu_0 m_i N_0}$; The time and length are normalized by the inverse of the solar wind ion gyrofrequency ($\Omega_{i0}^{-1} = m_i \,/\, eB_0$) and ion inertial length $d_{i0} = c \,/\, \omega_{pi0}$ (where $\omega_{pi0} = \left(N_0 e^2 \,/\, m_i \varepsilon_0\right)^{1/2}$ is ion plasma frequency) in the solar wind, respectively. To accommodate to the available computation resources, the solar wind ion inertial length d_{i0} in our simulations is several times larger than the realistic value. It was already observed that this kind of scaling does not affect the global structure of the magnetosphere (e.g., Omidi et al., 2004; Tóth et al., 2017).

Note that Case 1 in this paper is the same as Case 3 in Guo et al. (2021), in which the FR coalescence has been well identified. Moreover, the simulation domain of Case 1 contains a small dayside cusp region, and it is not enough to simulate the re-reconnection between FR and the cusp field lines. Therefore, Case 1 is used to study the re-reconnection process during the FR coalescence; Case 2 has a higher grid resolution and a larger simulation domain, which contains a larger dayside cusp region than Case 1. Therefore, although there is still re-reconnection between the FR and the cusp magnetic fields in Case 1, Case 2 is more suitable for studying this re-reconnection process. Note that we use a large B_y in Case 2, and this is because we want to study this process exclusively without any interference from other processes such as FR coalescence, and previous simulations have shown that a large B_y can eliminate FR coalescence (Guo et al., 2021).

3. Simulation Results

3.1. Detailed Coalescence Process of Magnetopause Flux Ropes (Case 1)

The FRs begin to form at the magnetopause at about $\Omega_{i0}t = 15$ due to the magnetopause multiple X line reconnection between IMF and the Earth's dipole field. Figure 1 shows the ion plasma density N_i near the noon-midnight meridian plane at $\Omega_{i0}t = 25$ and 35 obtained from Case 1. 3-D magnetic field lines are also plotted to show the FRs. There are about six FRs that exist at $\Omega_{i0}t = 25$–35, and only four FRs are shown in Figure 1. The green FR gradually moves northward and disappears in the cusp at $\Omega_{i0}t = 35$. FR_1 and FR_2 coalesce because FR_1 moves poleward faster than FR_2 during this time. The plasma density enhancement is evident in every FR, and the coalescence of FR_1 and FR_2 facilitates the combination of plasma within them.

Each FR has four topologies of magnetic field lines in terms of the magnetic connections to the magnetosphere (MSP) or to the IMF, and four topologies of field lines are MSP-MSP, IMF-MSP, MSP-IMF, and IMF-IMF field lines (Lee et al., 1993; Tan et al., 2011). The MSP-MSP field lines are closed field lines, the IMF-MSP and MSP-IMF field lines are semi-open field lines, and the IMF-IMF field lines are free field lines in FRs. To demonstrate the coalescence process more concisely, only the free field lines in the blue FR_1 and the semi-open field lines in the red FR_2 are shown in Figure 2a. Note that the blue and red FRs in Figures 2a and 3I are FR_1 and FR_2 in Figure 1, respectively. We first explain the topological changes of magnetic field lines in the coalescence process through the illustration Figure 3. In stage I of Figure 3, the middle of the blue FR_1 and the right end of the red FR_2 approach each other, and the reverse magnetic field directions between FR_1 and FR_2 trigger the re-reconnection between them. The re-reconnection results in the transformation of the blue free field lines into green semi-open field lines and yellow free field lines (Stage II). Finally, in stage III, the right half of the blue FR_1 splices to the right end of the red FR_2 to form the long green FR, and the left half of the blue FR_2 (yellow FR in stage III) gradually moves away.

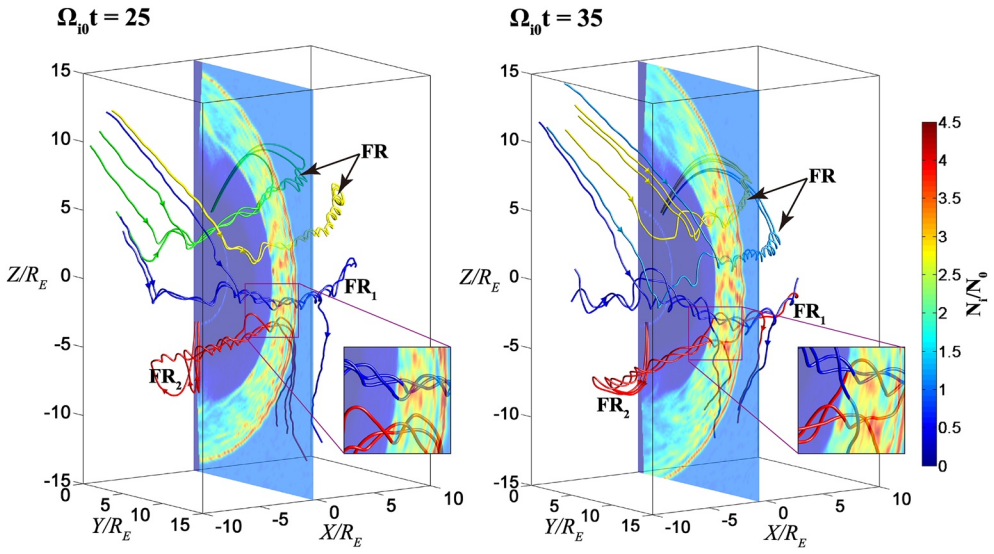

Figure 1. The distribution of the plasma density N_i near the noon-midnight meridian plane obtained from Case 1 at $\Omega_{i0}t = 25$ and 35. The right of each panel is a zoom-in view. One color represents one flux rope (FR), that is, there are green, yellow, blue, red, and sky-blue FRs in this figure. The letters and arrows represent the FRs.

As shown in Figure 2, the FR coalescence region is about $5R_E$ (about $-4R_E$–$1R_E$) in dawn-dusk direction. In Figure 2b, just as it is shown in Figure 3, a blue free field line reconnects with a red semi-open field line to form a green semi-open field line and a yellow free field line. The green field lines extend from FR_2 to FR_1, while the yellow field lines only occupy the left half of FR_1. The similar coalescence process is repeated until the coalescence is completed (see Figures 2b–2d). The green FR FR_{2_coal} composed of semi-open field lines and the yellow FR FR_{1_coal} composed of free field lines are formed eventually. The yellow FR (FR_{1_coal} in Figure 2d) is shorter than the blue FR (FR_1 in Figure 2a), and the green FR (FR_{2_coal} in Figure 2d) is longer than the red FR (FR_2 in Figure 2a). It is the FR coalescence that causes the change in length of FRs.

Figure 2e shows all possible topologies of magnetic field lines in FR_1 and FR_2. The blue field lines are free field lines and the sky-blue field line is a semi-open field line in FR_1. Moreover, the red field lines are semi-open field lines and the magenta field line is a free field line in FR_2. To avoid confusion, Figures 2a–2d only shows the reconnection between free field lines in FR_1 and semi-open field lines in FR_2. Table 1 lists all possible topological changes of magnetic field lines in FRs during this re-reconnection process. The color of texts corresponds to the color of FRs in Figures 2a–2d. For example, for Type 1, the semi-open field lines in FR_1 reconnect with the semi-open field lines in FR_2 to form the semi-open field lines in FR_{1_coal} and the semi-open field lines in FR_{2_coal}. Type 3 in Table 1 represents the re-reconnection process which is shown in Figures 2 and 3. Because the closed field lines in FR_1 and FR_2 are rare, we do not consider them.

Previous simulation studies for magnetopause FR coalescence are based on 2-D global hybrid simulations: two FRs move close to each other and coalesce to form a bigger one (Hoilijoki et al., 2017; Sibeck & Omidi, 2012). However, in Figure 2d, from a 3-D perspective, the two FRs FR_{1_coal} and FR_{2_coal} are far apart, and the coalescence of FRs is over. Therefore, after the final 3-D coalescence is completed at $\Omega_{i0}t = 45$, two FRs FR_{1_coal} and FR_{2_coal} remain (see Figure 2d).

3.2. Reconnection Between Magnetopause Flux Ropes and Cusp Field Lines (Case 2)

Figure 4 shows the 3-D structure of FRs (only some of all FRs) obtained from Case 2 at $\Omega_{i0}t = 40$, and each of them is composed of helical magnetic field lines (Lee & Fu, 1985). The presence of IMF B_y breaks the magnetic symmetry (dawn-dusk) of magnetopause in default. Therefore, the FRs' axis tilts relative to the equatorial plane (Guo et al., 2021; Lee et al., 1993) and the dawn-dusk distribution of FRs is asymmetry. FRs are mainly concentrated on the dawn side in the northern hemisphere and on the dusk side in the southern hemisphere. The sky-blue FR FR_3 is our main subject of study.

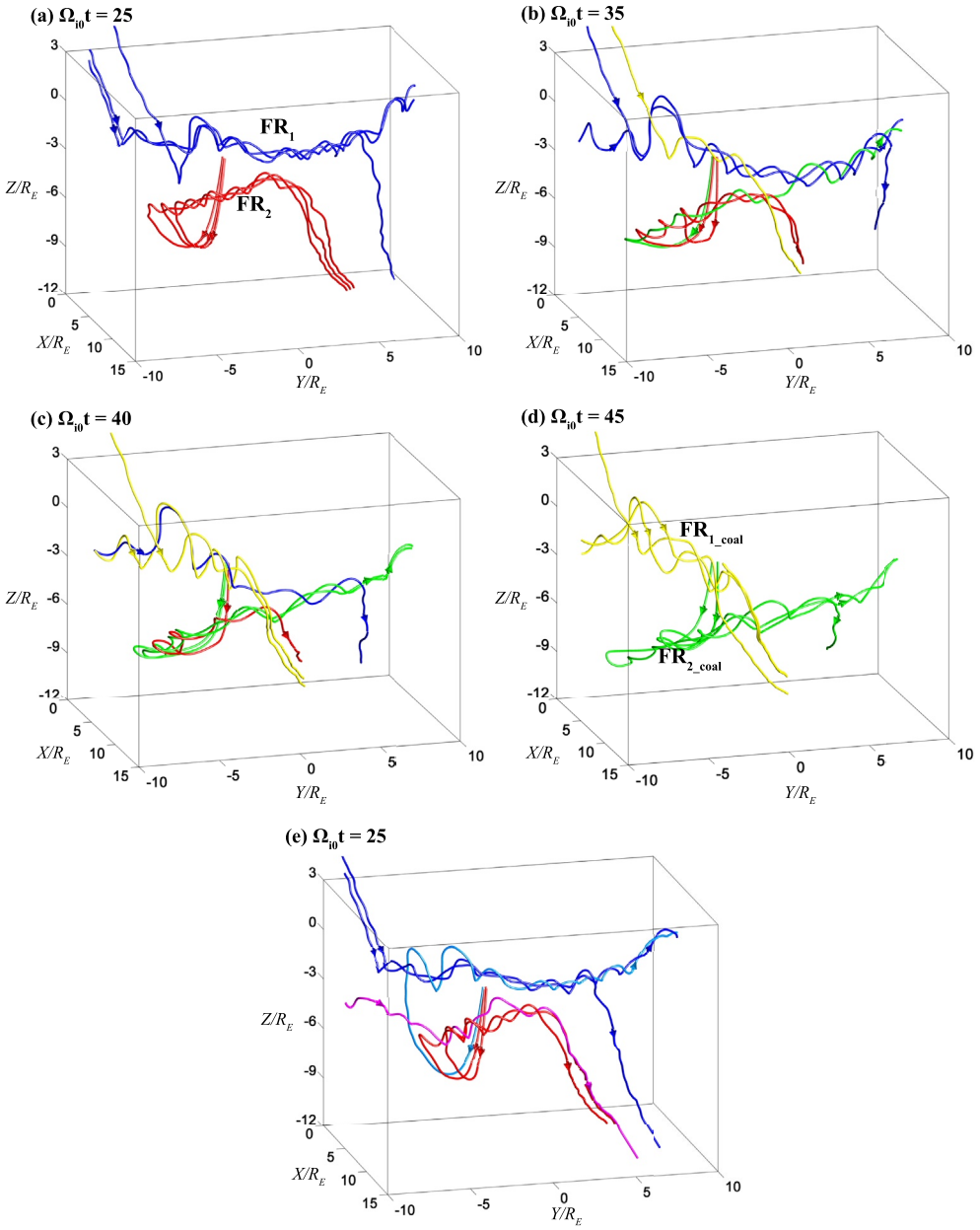

Figure 2. (a)–(d) Detailed coalescence process of blue flux rope (FR) FR_1 and red FR FR_2 obtained from Case 1 at $\Omega_{i0}t = 25$, 35, 40, and 45. The blue free field lines reconnect with the red semi-open field lines to form the yellow free field lines and the green semi-open field lines. Two FRs (yellow and green) remain after the coalescence at $\Omega_{i0}t = 45$. (e) All possible topologies of magnetic field lines in FR_1 and FR_2. Two blue free field lines and a sky-blue semi-open field line in FR_1; Two red semi-open field lines and a magenta free field line in FR_2.

As FRs are moving toward the cusp, V_z is not the same everywhere along the axis of FRs. Just as shown in Figures 5a and 5b (obtained from Case 2), V_z has a significant enhancement near ($6.8R_E$, $3.2R_E$) in the X-Y plane, and this part of FR will move faster toward cusp: the FR_3 is undergoing axial bending. When the FR_3 enters the cusp, the re-reconnection between this FR and the cusp field lines is triggered. As shown in Figure 5c, there is an obvious plasma jet from the reconnection X line into the magnetosheath and cusp. In the region where V_z is relatively large along the FR_3's axis, the re-reconnection is stronger due to the faster inflow.

In Figure 6, we show the topological changes of two magnetic field lines (orange free field line and sky-blue semi-open field lines) in FR_3 during the re-reconnection. The magnetic field lines in FR are in the opposite

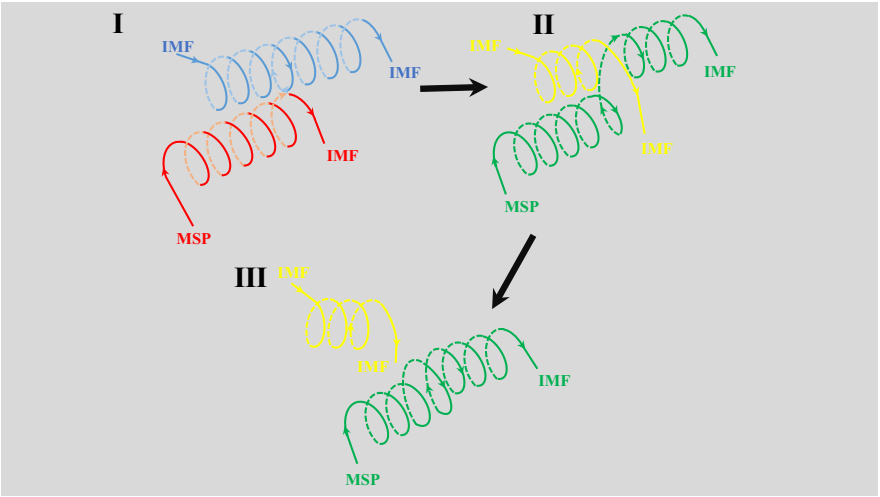

Figure 3. Schematic illustration for the re-reconnection (the coalescence of flux ropes [FRs]) process between free field lines in blue FR FR_1 and semi-open field lines in red FR FR_2.

direction to those in cusp, and reconnection is triggered. In part I, the orange free field lines reconnect with the black cusp field lines to form the red semi-open field lines and the green free field lines. In part II, the red and magenta semi-open field lines are formed by the reconnection between the sky-blue semi-open field lines and the black cusp field lines.

The above re-reconnection process is also confirmed by our simulation results. In Figure 7, the FR_3 is composed of sky-blue semi-open field lines and orange free field lines. The orange free field lines are reconnected to form the red semi-open field line and the green free field line at $\Omega_{i0}t = 85$. The two remaining sky-blue semi-open field lines also reconnect with the cusp field lines (not shown) to form the red and magenta semi-open field lines at $\Omega_{i0}t = 95$, and 105. Note that there is no obvious sequence of the two topological changes of field lines in FR_3. In the process of re-reconnection, the long FR FR_3 breaks into two short FRs FR_{3L} and FR_{3R} ($\Omega_{i0}t = 105$). The left FR FR_{3L} is near the noon-midnight meridian plane and the right FR FR_{3R} is on the dusk side. Regarding the fate of the FR_{3L} and FR_{3R}, FR_{3L}'s helical structure collapses gradually, and FR_{3R} gradually moves tailward out of the simulation region.

4. Conclusions and Discussion

Using 3-D global hybrid simulations, we examine the re-reconnection processes of magnetopause FRs. The main conclusions are presented below:

1. When an FR runs into another, the two FRs can coalesce and form two new FRs through a re-reconnection process. The re-reconnection between the two FRs (i.e., the coalescence of FRs) results in a transformation of free field lines into semi-open field lines and free field lines. The coalescence is essentially 3-D, with the interact region limited to several Earth radii in the dawn-dusk direction.
2. When an FR enters the cusp, the re-reconnection between the FR and the cusp field lines can be triggered, which forms an obvious plasma jetting from the re-reconnection X line into the magnetosheath and cusp. In the re-reconnection process, a free field line of FR reconnects with the cusp field line to form a semi-open field line and a free field line, and a semi-open field line of FR reconnects with the cusp field line to form two semi-open field lines. This process is also 3-D, and when the re-reconnection occurs strongly at the middle part of the FR, the FR can break into two short ones.

Table 1
Four Possible Topological Changes of Magnetic Field Lines During the Coalescence of FR_1 and FR_2

	Before coalescence		After coalescence	
	FR_1	FR_2	FR_{1_coal}	FR_{2_coal}
Type 1	Semi-open	Semi-open	Semi-open	Semi-open
Type 2	Semi-open	Free	Semi-open	Free
Type 3	Free	Semi-open	Free	Semi-open
Type 4	Free	Free	Free	Free

Note. Type 3 is presented in Figures 2a–2d, and the colors correspond to the color of the field lines in Figures 2a–2d, respectively. Closed field lines in FR_1 and FR_2 are rare, so we do not consider them.

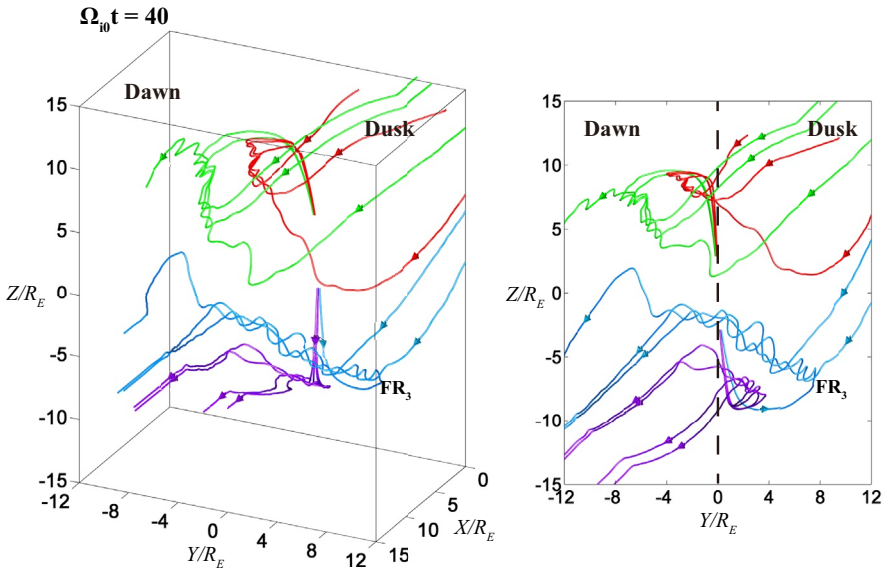

Figure 4. The structure of flux ropes (FRs) (only part of all FRs) obtained from Case 2 is shown in this figure. The left panel is from a 3-D perspective and the right panel is on the Y-Z plane. One color represents one FR, that is, there are red, green, sky-blue, and purple FRs in this figure. The dotted line in the right panel represents the noon-midnight meridian plane.

3. The coalescence of FRs allows the plasma in FRs to enter the Earth's magnetosphere along the newly formed semi-open field lines, and the re-reconnection between FRs and cusp field lines produces more semi-open field lines connected to the FRs. As a result, the two re-reconnection processes favor particles and energy transport toward the Earth's magnetosphere.

In the previous 2-D simulation studies, the coalescence of FRs is simply considered as the fusion of two magnetic islands into one (e.g., Hoilijoki et al., 2017; Oka et al., 2010; Pritchett, 2008; Sibeck & Omidi, 2012). However, in 3-D, there are still two FRs after the coalescence because the coalescence occurs only in a limited region in the dawn-dusk direction (see Figure 2). Therefore, it is not appropriate to examine the 3-D FR coalescence from a 2-D perspective. Likewise, the re-reconnection between the FRs and the cusp magnetic field lines is also 3-D. Omidi and Sibeck (2007) studied this process in 2-D. Here our simulations show that, in 3-D, the re-reconnection does not just occur in the noon-midnight meridian plane but occurs almost across the entire FR. Moreover, the middle part of FR has a strong re-reconnection due to faster inflow V_z, which can cause the FR to break into two short ones (see Figures 5 and 7).

The structure and coalescence of magnetopause FRs have been studied previously by 3-D global-scale simulations, mostly using magnetohydrodynamic (MHD) models (e.g., Dorelli & Bhattacharjee, 2009; Fedder et al., 2002; Glocer et al., 2016; Raeder, 2006; Winglee et al., 2008). However, these MHD simulations do not include particle kinetics, so they cannot describe the small, kinetic-scale FRs at the magnetopause, not to mention the coalescence between them. More recently, using an MHD with embedded PIC simulation, Chen et al. (2017) showed the coalescence between two FRs but did not examine the topological changes during this process. Three-dimensional FR coalescence was also considered by Russell and Qi (2020) to be entanglement between two FRs, which was thereafter simulated by Jia et al. (2021) using a 3-D local Hall MHDs model. They suggested that two FRs can entangle and reconnect, producing a new pair of FRs with axis approximately perpendicular to each other. Our simulations in this paper show a similar process but in a global-scale, which can better reveal the nature of 3-D FR coalescence. The re-reconnection between two FRs results in topological change of magnetic field lines in two FRs, and a pair of FRs remain after the coalescence is completed. Most of the field lines in FR_1 and FR_2 are free and semi-open field lines, so in Figures 2 and 3 we only examine the topological changes of these two types of field lines. The other possible topological changes are fewer than the above two, so we do not show them in Figures 2 and 3 but list them

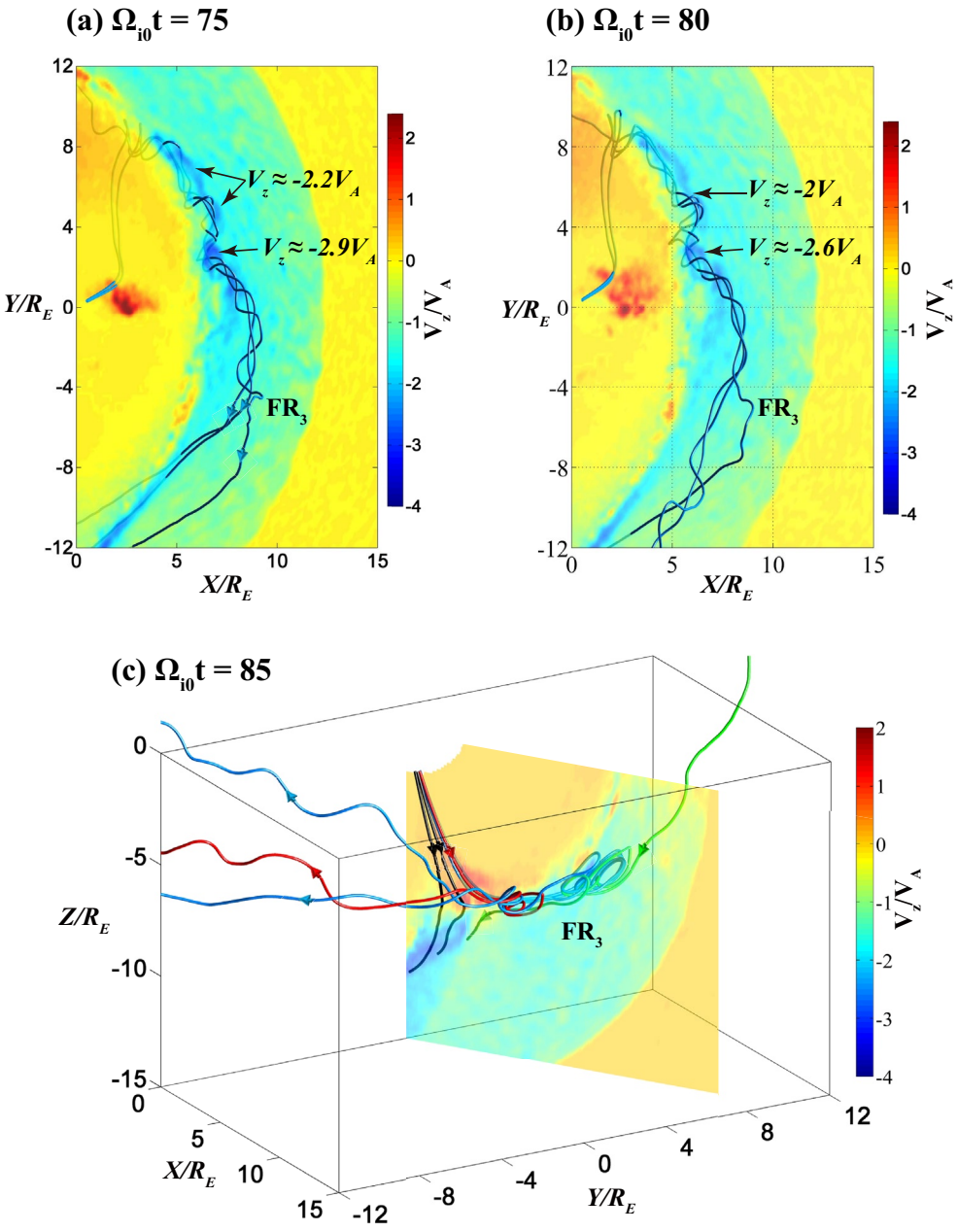

Figure 5. (a) The distribution of ion flow velocity V_z in $z = -6.8\ R_E$ plane obtained from Case 2 at $\Omega_{i0}t = 75$. (b) The distribution of ion flow velocity V_z in $z = -7.2\ R_E$ plane at $\Omega_{i0}t = 80$. (c) The distribution of ion flow velocity V_z in a plane rotated 32° around the z axis from the noon-midnight plane at $\Omega_{i0}t = 85$. The sky-blue flux rope (FR) FR_3 is the same as in Figure 4. Note that the red spot with high positive V_z in panel (a) and (b) is a plasma jet formed by the re-reconnection between FR and cusp field lines, which corresponds to the positive V_z in panel (c).

in Table 1. For example, for Type 1, the semi-open field line in one FR reconnects with the semi-open field line in another FR to form two semi-open field lines.

Dayside auroras are often produced by magnetic reconnection between the IMF and the terrestrial magnetic field (Frey et al., 2019). Magnetosheath plasma can enter the ionosphere along the semi-open magnetic field lines formed by the magnetopause reconnection and produce auroral phenomena (Lockwood et al., 1993). Our results can help understand an important auroral signature in the ionosphere-poleward moving auroral forms (PMAFs). PMAFs were first observed by Vorobjev et al. (1975). Typical PMAFs usually brighten

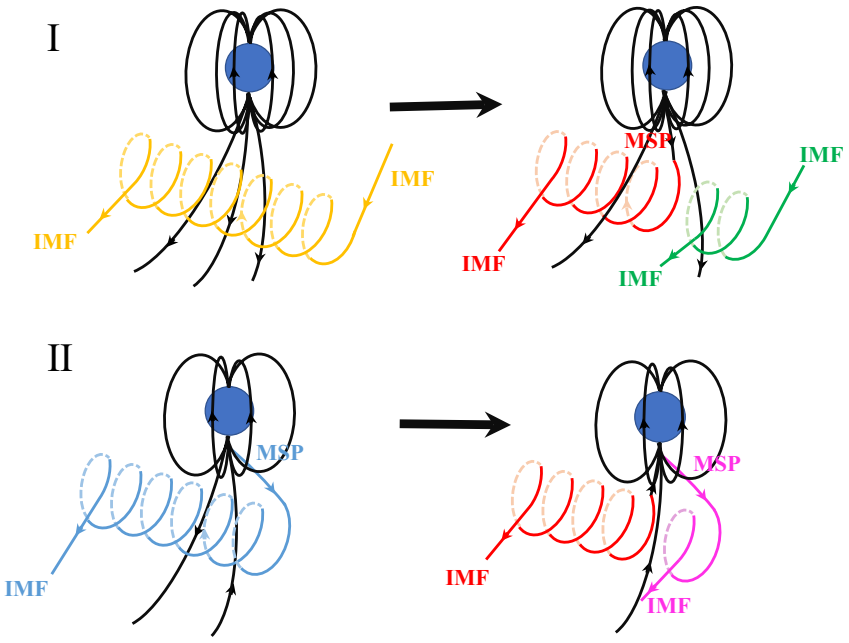

Figure 6. Schematic illustration for the re-reconnection process between orange free field lines (sky-blue semi-open field lines) in FR_3 and black cusp field lines. (a) the orange free field line reconnects with the black cusp field line to form the red semi-open field line and the green free field line. (b) the sky-blue semi-open field line reconnects with the black cusp field line to form the red and magenta semi-open field line.

near the equatorward boundary of the dayside auroral oval (equatorward boundary intensification or EBI), gradually move poleward, and fade away eventually (e.g., Sandholt et al., 1986). The recurrence period of PMAFs is generally 5–15 min and each PMAF lasts for 2–10 min (Sandholt et al., 1986). About 70% of PMAFs form about 8 min after an IMF southward turning (Wang, Nishimura, et al., 2016). The formation condition, recurrence period, lifetime, and motion of PMAFs are very similar to magnetopause FRs, and thus PMAFs are considered to be a possible ionospheric signature of magnetopause reconnection (e.g., Fasel et al., 1992, 1993; Hwang et al., 2020; Sandholt & Farrugia, 2007). The formation of FR_1 and FR_2 in Case 1 can lead to the onset of PMAFs (PMAF1 and PMAF2) in the ionosphere (Lee & Fasel, 1994; Omidi & Sibeck, 2007), and the movement of FR_1 and FR_2 toward the cusp corresponds to the poleward movement of PMAFs. The coalescence of FR_1 and FR_2 may lead to the merging of the two PMAFs. The PMAF merge may be similar to the FR coalescence process, with two PMAFs remaining, and the higher latitude PMAF becoming longer (see Figure 2). However, there is no observation of PMAFs indicating the presence of PMAF merge. Therefore, this idea deserves to be confirmed by future observations combining magnetopause FRs and the ionospheric auroras.

What's more, recent high-resolution observations provide evidence that one PMAF could correspond to double FRs, that is, one PMAF is not necessarily corresponding to only one FR (Taguchi et al., 2012). The FRs in Case 2 can break into two parts due to non-uniform re-reconnection (see Figures 5 and 7), and the corresponding PMAF may also break into two parts. This result could also account for one PMAF which corresponds to double FRs, which is observed by Taguchi et al. (2012).

Fasel et al. (1994) divided PMAFs into three categories based on their brightening history. The first category of PMAFs is relatively common, and when these PMAFs move into the polar cap, they gradually disappear. The second category of PMAFs can re-brighten as they move poleward, and the third category of PMAFs is similar to the former except that they stop moving during rebrightening. Omidi and Sibeck (2007) think the second and third categories of PMAFs are caused by bigger FRs with strong density enhancements which can reconnect with cusp field lines. In our simulation results, this re-reconnection process can produce more semi-open field lines connected to the FRs (see Figures 6 and 7). More semi-open field lines can allow more plasma from the solar wind enter into the Earth's ionosphere, which can trigger the rebrightening of

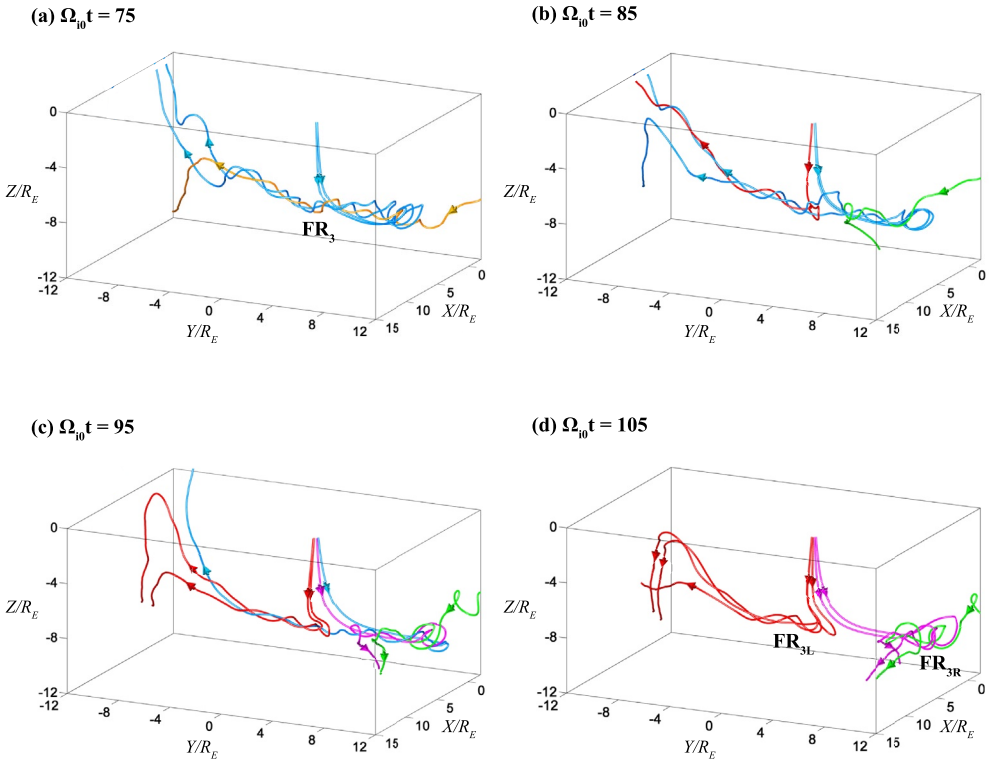

Figure 7. Detailed re-reconnection process of the sky-blue flux rope and the cusp field lines obtained from Case 2 at $\Omega_{i0}t$ = 75, 85, 95, and 105. The orange free field lines reconnect with the cusp field lines to form the red semi-open field lines and the green free field lines. The sky-blue semi-open field lines reconnect with the cusp field lines to form the red semi-open field lines and the magenta semi-open field lines.

the PMAFs. The combined study of magnetopause FRs and ionospheric PMAFs allows us to better understand the solar wind-Earth's magnetosphere coupling.

Data Availability Statement

The simulation results described in Section 3 are generated from our computer simulation model. Moreover, the simulation model is described in Section 2. In this paper, the simulation data which is used to plot the figures all can be downloaded from https://doi.org/10.12176/01.99.00374.

Acknowledgments
This research was funded by the Key Research Program of Frontier Sciences CAS (QYZDJ-SSW-DQC010), NSFC grant 41774169, and the Strategic Priority Research Program of Chinese Academy of Sciences Grant No. XDB41000000. The authors gratefully acknowledge the data resources from the "National Space Science Data Center, National Science & Technology Infrastructure of China. (http://www.nssdc.ac.cn)."

References

Akhavan-Tafti, M., Slavin, J. A., Le, G., Eastwood, J. P., Strangeway, R. J., Russell, C. T., et al. (2018). MMS examination of FTEs at the earth's subsolar magnetopause. *Journal of Geophysical Research: Space Physics*, *123*, 1224–1241. https://doi.org/10.1002/2017JA024681

Alm, L., Farrugia, C. J., Paulson, K. W., Argall, M. R., Torbert, R. B., Burch, J. L., et al. (2018). Differing properties of two ion-scale magnetopause flux ropes. *Journal of Geophysical Research: Space Physics*, *123*, 114–131. https://doi.org/10.1002/2017JA024525

Che, H., Drake, J. & Swisdak, M. (2011). A current filamentation mechanism for breaking magnetic field lines during reconnection. *Nature*, *474*, 184–187. https://doi.org/10.1038/nature10091

Chen, Y., Tóth, G., Cassak, P., Jia, X., Gombosi, T. I., Slavin, J. A., et al. (2017). Global three-dimensional simulation of earth's dayside reconnection using a two-way coupled magnetohydrodynamics with embedded particle-in-cell model: Initial results. *Journal of Geophysical Research: Space Physics*, *122*, 10318–10335. https://doi.org/10.1002/2017JA024186

Dorelli, J. C., & Bhattacharjee, A. (2009). On the generation and topology of flux transfer events, *Journal of Geophysical Research*, *114*, A06213. https://doi.org/10.1029/2008JA013410

Fasel, G. I., Minow, J. I., Smith, R. W., Deehr, C. S., & Lee, L. C. (1992). Multiple brightenings of transient dayside auroral forms during oval expansions. *Geophysical Research Letters*, *19*(24), 2429–2432. https://doi.org/10.1029/92GL02103

Fasel, G. J., Lee, L. C., & Smith, R. W. (1993). A mechanism for the multiple brightenings of dayside poleward-moving auroral forms, *Geophysical Research Letters*, *20*(20), 2247–2250. https://doi.org/10.1029/93GL02487

Fasel, G. J., Minow, J. I., Lee, L. C., Smith, R. W., & Deehr, C. S. (1994). *Poleward-moving auroral forms: What do we really know about them? Physical signatures of magnetospheric boundary layer processes*. eds., In J. A. Holtet and A. Egeland (pp. 211–216). New York: Springer.

Fedder, J. A., Slinker, S. P., Lyon, J. G., & Russell, C. T. (2002). Flux transfer events in global numerical simulations of the magnetosphere. *Journal of Geophysical Research*, *107*(A5), 1048. https://doi.org/10.1029/2001JA000025

Frey, H. U., Han, D., Kataoka, R., Lessard, M. R., Milan, S. E., Nishimura, Y., et al. (2019). Dayside aurora. *Space Science Reviews*, *215*, 51. https://doi.org/10.1007/s11214-019-0617-7

Fuselier, S. A., Petrinec, S. M., Trattner, K. J., Broll, J. M., Burch, J. L., Giles, B. L., et al. (2018). Observational evidence of large-scale multiple reconnection at the earth's dayside magnetopause. *Journal of Geophysical Research: Space Physics*, *123*, 8407–8421. https://doi.org/10.1029/2018JA025681

Glocer, A., Dorelli, J., Toth, G., Komar, C. M., & Cassak, P. A. (2016). Separator reconnection at the magnetopause for predominantly northward and southward IMF: Techniques and results, *Journal of Geophysical Research: Space Physics*, *121*, 140–156. https://doi.org/10.1002/2015JA021417

Guo, J., Lu, S., Lu, Q., Lin, Y., Wang, X., Huang, K., et al. (2021). Structure and coalescence of magnetopause flux ropes and their dependence on IMF clock angle: Three-dimensional global hybrid simulations. *Journal of Geophysical Research: Space Physics*, *126*, e2020JA028670. https://doi.org/10.1029/2020JA028670

Guo, Z., Lin, Y., Wang, X., Vines, S. K., Lee, S. H., & Chen, Y. (2020). Magnetopause reconnection as influenced by the dipole tilt under southward IMF conditions: Hybrid simulation and MMS observation. *Journal of Geophysical Research: Space Physics*, *125*, e2020JA027795. https://doi.org/10.1029/2020JA027795

Hasegawa, H., Wang, J., Dunlop, M. W., Pu, Z. Y., Zhang, Q.-H., Lavraud, B., et al. (2010). Evidence for a flux transfer event generated by multiple X-line reconnection at the magnetopause. *Geophysical Research Letters*, *37*, L16101. https://doi.org/10.1029/2010GL044219

Hoilijoki, S., Ganse, U., Pfau-Kempf, Y., Cassak, P. A., Walsh, B. M., Hietala, H., et al. (2017). Reconnection rates and X line motion at the magnetopause: Global 2D-3V hybrid-Vlasov simulation results. *Journal of Geophysical Research: Space Physics*, *122*, 2877–2888. https://doi.org/10.1002/2016JA023709

Hwang, K.-J., Nishimura, Y., Coster, A. J., Gillies, R. G., Fear, R. C., Fuselier, S. A., et al. (2020). Sequential observations of flux transfer events, poleward moving auroral forms, and polar cap patches. *Journal of Geophysical Research: Space Physics*, *125*, e2019JA027674. https://doi.org/10.1029/2019JA027674

Jia, Y.-D., Qi, Y., Lu, S., & Russell, C. T. (2021). Temporal evolution of flux rope/tube entanglement in 3-D Hall MHD simulations. *Journal of Geophysical Research: Space Physics*, *126*, e2020JA028698. https://doi.org/10.1029/2020JA028698

Kacem, I., Jacquey, C., Génot, V., Lavraud, B., Vernisse, Y., Marchaudon, A., et al. (2018). Magnetic reconnection at a thin current sheet separating two interlaced flux tubes at the earth's magnetopause. *Journal of Geophysical Research: Space Physics*, *123*, 1779–1793. https://doi.org/10.1002/2017JA024537

Kuznetsova, M. M., Hesse, M., & Winske, D. (1998). Kinetic quasi-viscous and bulk flow inertia effects in collisionless magnetotail reconnection, *Journal of Geophysical Research*, *103*(A1), 199–213. https://doi.org/10.1029/97JA02699

Lee, L. C., & Fasel, G. J. (1994). *Physical signatures of magnetospheric boundary layer processes* (pp 291–306). Springer Netherlands. https://doi.org/10.1007/978-94-011-1052-5_20

Lee, L. C., & Fu, Z. F. (1985). A theory of magnetic flux transfer at the Earth's magnetopause. *Geophysical Research Letters*, *12*, 105–108. https://doi.org/10.1029/GL012i002p00105

Lee, L. C., Ma, Z. W., Fu, Z. F., & Otto, A. (1993). Topology of magnetic flux ropes and formation of fossil flux transfer events and boundary layer plasmas. *Journal of Geophysical Research*, *98*(A3), 3943–3951. https://doi.org/10.1029/92JA02203

Lin, Y., & Wang, X. (2005). Three-dimensional global hybrid simulation of dayside dynamics associated with the quasi-parallel bow shock. *Journal of Geophysical Research*, *110*, A12216. https://doi.org/10.1029/2005JA011243

Lin, Y., & Wang, X. Y. (2006). Formation of dayside low-latitude boundary layer under northward interplanetary magnetic field. *Geophysical Research Letters*, *33*, L21104. https://doi.org/10.1029/2006GL027736

Lin, Y., Wang, X. Y., Lu, S., Perez, J. D., & Lu, Q. (2014). Investigation of storm time magnetotail and ion injection using three-dimensional global hybrid simulation. *Journal of Geophysical Research: Space Physics*, *119*, 7413–7432. https://doi.org/10.1002/2014JA020005

Lockwood, M., Carlson, H. C., & Sandholt, P. E. (1993). Implications of the altitude of transient 630 nm dayside auroral emissions. *Journal of Geophysical Research*, *98*(A9), 15571–15587. https://doi.org/10.1029/93JA00811

Øieroset, M., Phan, T. D., Haggerty, C., Shay, M. A., Eastwood, J. P., Gershman, D. J., et al. (2016). MMS observations of large guide field symmetric reconnection between colliding reconnection jets at the center of a magnetic flux rope at the magnetopause. *Geophysical Research Letters*, *43*, 5536–5544. https://doi.org/10.1002/2016GL069166

Oka, M., Phan, T.-D., Krucker, S., Fujimoto, M., & Shinohara, I. (2010). Electron acceleration by multi-island coalescence. *The Astrophysical Journal*, *714*, 915–926. https://doi.org/10.1088/0004-637X/714/1/915

Omidi, N., Blanco-Cano, X., Russell, C. T., & Karimabadi, H. (2004). Dipolar magnetospheres and their characterization as a function of magnetic moment, *Advances in Space Research*, *33*, 1996–2003. https://doi.org/10.1016/j.asr.2003.08.041

Omidi, N., & Sibeck, D. G. (2007). Flux transfer events in the cusp, *Geophysical Research Letters*, *34*, L04106. https://doi.org/10.1029/2006GL028698

Pritchett, P. L. (2008). Energetic electron acceleration during multi-island coalescence. *Physics of Plasmas*, *15*, 102105. https://doi.org/10.1063/1.2996321

Raeder, J. (2006). Flux transfer events: 1. Generation mechanism for strong southward IMF. *Annales Geophysicae*, *24*(1), 381–392. https://doi.org/10.5194/angeo-24-381-2006

Ruffenach, A., Lavraud, B., Owens, M. J., Sauvaud, J.-A., Savani, N. P., Rouillard, A., et al. (2012) Multispacecraft observation of magnetic cloud erosion by magnetic reconnection during propagation, *Journal of Geophysical Research*, *117*, A09101. https://doi.org/10.1029/2012JA017624

Russell, C. T., & Elphic, R. C. (1978) Initial ISEE magnetometer results: Magnetopause observations. *Space Science Reviews*, *22*, 681–715. https://doi.org/10.1007/BF00212619

Russell, C. T., & Qi, Y. (2020). Flux ropes are born in pairs: An outcome of interlinked, reconnecting flux tubes. *Geophysical Research Letters*, *47*, e2020GL087620. https://doi.org/10.1029/2020GL087620

Sandholt, P. E., Deehr, C. S., Egeland, A., Lybekk, B., Viereck, R., Romick, G. J. (1986). Signatures in the dayside aurora of plasma transfer from the magnetosheath. *Journal of Geophysical Research*, *91*(A9), 10063–10079. https://doi.org/10.1029/JA091iA09p10063

Sandholt, P. E., & Farrugia, C. J. (2007). Poleward moving auroral forms (PMAFs) revisited: Responses of aurorae, plasma convection and Birkeland currents in the pre- and postnoon sectors under positive and negative IMF B_y conditions. *Annales Geophysicae*, *25*(7), 1629–1652. https://doi.org/10.5194/angeo-25-1629-2007

Sibeck, D. G., & Omidi, N. (2012). Flux transfer events: Motion and signatures. *Journal of Atmospheric and Solar-Terrestrial Physics*, *87*, 20–24. https://doi.org/10.1016/j.jastp.2011.07.010

Swift, D. W. (1996). Use of a hybrid code for global-scale plasma simulation. *Journal of Computational Physics*, *126*(1), 109–121. https://doi.org/10.1006/jcph.1996.0124

Taguchi, S., Hosokawa, K., Ogawa, Y., Aoki, T., & Taguchi, M. (2012). Double bursts inside a poleward-moving auroral form in the cusp. *Journal of Geophysical Research*, *117*, A12301. https://doi.org/10.1029/2012JA018150

Tan, B., Lin, Y., Perez, J. D., & Wang, X. Y. (2011). Global-scale hybrid simulation of dayside magnetic reconnection under southward IMF: Structure and evolution of reconnection, *Journal of Geophysical Research*, *116*, A02206. https://doi.org/10.1029/2010JA015580

Tan, B., Lin, Y., Perez, J. D., & Wang, X. Y. (2012). Global-scale hybrid simulation of cusp precipitating ions associated with magnetopause reconnection under southward IMF. *Journal of Geophysical Research*, *117*, A03217. https://doi.org/10.1029/2011JA016871

Tóth, G., Chen, Y., Gombosi, T. I., Cassak, P., Markidis, S., & Peng, I. B. (2017). Scaling the ion inertial length and its implications for modeling reconnection in global simulations. *Journal of Geophysical Research: Space Physics*, *122*, 10336–10355. https://doi.org/10.1002/2017JA024189

Vorobjev, V. G., Gustafsson, G., Starkov, G. V., Feldstein, Y. I., & Shevnina, N. F. (1975). Dynamics of day and night aurora during substorms. *Planetary and Space Science*, *23*(2), 269–278. https://doi.org/10.1016/0032-0633(75)90132-4

Wang, B., Nishimura, Y., Zou, Y., Lyons, L. R., Angelopoulos, V., Frey, H., & Mende, S. (2016). Investigation of triggering of poleward moving auroral forms using satellite-imager coordinated observations. *Journal of Geophysical Research: Space Physics*, *121*, 10929–10941. https://doi.org/10.1002/2016JA023128

Wang, H. Y., Lu, Q. M., Huang, C., & Wang, S. (2016). The mechanisms of electron acceleration during multiple X line magnetic reconnection with a guide field. *The Astrophysical Journal*, *821*, 84. https://doi.org/10.3847/0004-637X/821/2/84

Wang, R. S., Lu, Q. M., Nakamura, R., Baumjohann, W., Russell, C. T., Burch, J. L., et al. (2017). Interaction of magnetic flux ropes via magnetic reconnection observed at the magnetopause. *Journal of Geophysical Research: Space Physics*, *122*, 10436–10447. https://doi.org/10.1002/2017JA024482

Wang, R. S., Lu, Q. M., Nakamura, R., Huang, C., Du, A. M., Guo, F., et al. (2016). Coalescence of magnetic flux ropes in the ion diffusion region of magnetic reconnection. *Nature Physics*, *12*(3), 263–267. https://doi.org/10.1038/Nphys3578

Winglee, R. M., Harnett, E., Stickle, A., & Porter, J. (2008). Multiscale/multifluid simulations of flux ropes at the magnetopause within a global magnetospheric model. *Journal of Geophysical Research*, *113*, A02209. https://doi.org/10.1029/2007JA012653

Zhong, J., Pu, Z. Y., Dunlop, M. W., Bogdanova, Y. V., Wang, X. G., Xiao, C. J., et al. (2013). Three-dimensional magnetic flux rope structure formed by multiple sequential X-line reconnection at the magnetopause. *Journal of Geophysical Research: Space Physics*, *118*, 1904–1911. https://doi.org/10.1002/jgra.50281

Zhou, M., Berchem, J., Walker, R. J., El-Alaoui, M., Deng, X., Cazzola, E., et al. (2017). Coalescence of macroscopic flux ropes at the subsolar magnetopause: Magnetospheric multiscale observations. *Physical Review Letters*, *119*, 055101. https://link.aps.org/doi/10.1103/PhysRevLett.119.055101

Zong, Q.-G., Fritz, T. A., Pu, Z. Y., Fu, S. Y., Baker, D. N., Zhang, H., et al. (2004). Cluster observations of earthward flowing plasmoid in the tail, *Geophysical Research Letters*, *31*, L18803. https://doi.org/10.1029/2004GL020692